PHYSICAL REVIEW B VOLUME 11, NUMBER 4 15 FEBRUARY 1975

Far-infrared absorption in small metallic particles*

D. B. Tanner† and A. J. Sievers
Laboratory of Atomic and Solid State Physics, Cornell University, Ithaca, New York 14850

R. A. Buhrman
School of Applied and Engineering Physics, Cornell University, Ithaca, New York 14850

(Received 29 April 1974)

Far infrared transmission measurements were made on powder samples of Cu, Al, Sn, and Pb. The diameter of the particles ranged from 65 to 350 Å. All of the samples showed absorption which was very small at low frequencies and which increased more or less linearly as the frequency increased. There was no change in the absorption as the temperature was varied from 1.2 to 20 K. For the smaller particles absorption curves calculated from the modified theory of Gor'kov and Eliashberg give a good description of the data, although clear choices between different energy-level ensembles cannot be made. Our measurements provide direct evidence that, for superconducting particles of diameter ~ 100 Å and mean energy-level spacing $\sim k T_c$, the energy gap structure in the density of states is either much attenuated or is completely absent.

I. INTRODUCTION

This paper describes experiments on the far-infrared absorption in small metallic particles. The particle size is less than any characteristic lengths (mean free path, penetration depth, coherence length) in the bulk metal but larger than a lattice constant and so approximates a zero-dimensional metal.

Fröhlich[1] was the first to point out that the conduction electrons in small metallic particles inhabit quantized energy levels. Kubo[2] showed that the mean energy-level spacing at the Fermi surface Δ is just the inverse of the density of states for one spin direction of the free electron gas

$$\Delta = 2\pi^2\hbar^2/\Omega m^* k_F = \tfrac{4}{3} E_F/N \quad , \tag{1}$$

where Ω is the volume of the particle, m^* is the effective mass of the electrons, N is the number of free electrons in the particle, and k_F and E_F are the Fermi momentum and energy.

The problem of averaging over ensembles of randomly separated energy levels has been extensively studied for the case of level statistics in large nuclei. Dyson[3] discussed this for various symmetries; he found three distinct ensembles. Gor'kov and Eliashberg[4] applied these to the case of small metallic particles to calculate, among other things, the electromagnetic response.

Infrared measurements[5] on small particles have already been reported for the frequency much larger than the mean energy-level spacing Δ. This paper describes the first measurements of the absorption in small particles at frequencies comparable with the mean energy spacing.

In Sec. II we discuss the experimental techniques for sample preparation and far-infrared measurements. In Sec. III the far-infrared results are presented. Calculations appropriate to a classical and also to a nonclassical description are developed in Sec. IV and compared with the experimental data in Sec. V. For the smaller particles, curves generated from the theory of Gor'kov and Eliashberg, with the depolarization field taken care of correctly, give a good description of the data.

II. EXPERIMENTAL TECHNIQUES

There were two methods that were used to prepare the small particles investigated in this study. The first method was a colloidal technique which produced a so-called small-particle sludge. This technique used the Svedberg method of electrical condensation of metal in a liquid medium.[6,7] The method consists simply of striking high-frequency arcs between chips of metal under a polar liquid. The electrical arcs vaporize metal from the chips. This vapor condenses in the liquid and goes into suspension as very small colloidal particles. Larger particles that are formed from molten metal will settle out if the liquid is left standing for a few hours. Using a Lepel high-voltage rf power supply operating at 450 kHz, stable copper and lead colloidal dispersions in acetone were obtained in this manner. The small-particle sludge was obtained from this dispersion by spraying the liquid onto a heated quartz disk. The spraying was done slowly so that liquid did not collect on the quartz. In this way, thick and relatively uniform layers of the aptly named sludge could be prepared.

The second small-particle preparation technique was the evaporation of high-purity metal in an inert-gas atmosphere.[8,9] With this technique, very small high-quality generally single-crystal particles can be readily produced. The particles grow in the gas from the atomic vapor and are then de-

posited on nearby collecting surfaces. This is the method used by Harris and Beasley in producing their gold-smoke deposits.[5] The mean size of the particles depends upon the inert-gas pressure, the atomic mass of the gas, and the evaporation rate. By varying these parameters a range of metal particle sizes can be obtained.

To ensure electrical insulation between the metal particles produced in this manner, it was necessary to slowly admit a small amount of oxygen to the vacuum chamber during the evaporation. The oxide coating that then formed on the surfaces of the particles electrically isolated the particles from each other on a macroscopic scale as measured by an ohmmeter and on a microscopic scale, at least for aluminum and tin particles, as indicated by their superconducting diamagnetic transition.[10]

Following an evaporation, the metal smoke was collected by brushing it from the surfaces upon which it had deposited in the vacuum chamber. This smoke deposit was then clamped between two sheets of polyethylene, using a ring cut from a plastic vial as a spacer.

The far-infrared spectra were all recorded using a lamellar grating interferometer[11] and a ^{3}He-cooled germanium bolometer detector.[12] As many as four specimens (and one empty sample holder) could be mounted on a rotating disk and moved one after the other, six-shooter fashion, into a gap in the light pipe carrying the radiation from the interferometer to the detector. A carbon resistor and heater were attached to the sample holder, to enable its temperature to be adjusted and measured.

During the course of these experiments far-infrared measurements were made on samples of carbon, copper, aluminum, tin, and lead. Table I gives the important data on these samples. The carbon was commercial lampblack, obtained from the Carbolac Corp.[13] All of the numbered metallic samples were made by the smoke method; the other two were sludge. The sample designation is in the first column of the table. In the second is the helium-gas pressure, in Torr, that was in the bell jar during the smoke evaporation. To make Al 3 the helium was replaced by argon.

The diameter is that determined by electron microscopy of the samples. For each smoke evaporation there were two electron microscope grids in the bell jar. These were examined under appropriate magnification and pictures were taken. From these the diameter and its variation could be found. The variation in size given in Table I is a plus or minus amount on the diameter. About 75% of the particles are within this range. The electron microscope grid for the copper sludge was prepared by placing a drop of the colloid on the grid and letting it dry. There were no pictures taken of the lead; its size is guessed to be about that of the copper. The last two columns in the table show the packing density or filling factor of the particles f and the number per unit volume. These are calculated from

$$f = W/\rho V\ , \quad N/V = 6f/\pi D^3 = f/\Omega\ ,$$

where ρ is the density of the bulk metal, W is the weight of the sample, V is its volume, and D is the diameter of the particles. It is interesting to note that the filling factor seems to be a function of the type of material rather than of the particle size.

There is one other important sample property that is not included in the table because it is the same in all samples. This is the electrical resistance of the samples which is in all cases greater than 100 MΩ at 300 K. This is the limit of the measuring apparatus and corresponds to a resistivity in the smoke of 10^6 Ω cm. Our particles are well isolated and should be distinguished from those contained in granular films where there is considerable tunneling between individual particles yielding resistivities on the order of 10^{-3}–10^{-4} Ω cm. This is an important distinction; particles which are closely connected by tunneling will show

TABLE I. Properties of small particles.

Sample	Helium pressure (Torr)	Diameter (Å)	Variation (Å)	Filling factor	Number density (10^{16} cm^{-3})
C	•••	90	•••	0.043	11
Pb sludge	•••	100	30	0.12	23
Cu sludge	•••	100	30	0.12	23
Cu 2	0.5	70	10	0.028	16
Cu 3	2.5	270	30	0.027	0.26
Al 1	0.5	150	12	0.040	2.3
Al 2	0.5	400	40	0.041	0.12
Al 3	2(Ar)	375	25	0.040	0.15
Sn 1	1	140	15	0.018	1.3
Sn 2	5	150	25	0.018	1.0

quite different superconducting properties as the Cooper pairs can easily pass from particle to particle. Size quantization will be affected also.

The typical weight of the samples was 0.01 to 0.03 g. This was spread over an area of 1.5 cm^2 so that the samples were 0.1 to 0.2 cm thick. Perhaps the most surprising result of these experiments is that metals of this thickness show large infrared transmissions.

III. FAR-INFRARED RESULTS

The absorption coefficient α in the far infrared is shown in Figures 1–6. It is defined as

$$\alpha = -(1/l)\ln I/I_0 \ ,$$

where I is the intensity transmitted through the sample; I_0 is the incident intensity, measured by replacing it with an empty sample holder; and l is its length. For small particles,

$$l = W/\rho f A \ ,$$

where W is the weight of the sample, A is its cross-sectional area, ρ is the density of the bulk metal, and f is the filling factor of the powder.

The plots are of absorption coefficient in cm^{-1} versus frequency in cm^{-1} along the bottom and Hz along the top. There has been one readjustment to the data. This arises because the detector shows a nonlinear response to the relatively large changes in background radiation which occur when the particles are placed into the far infrared beam. The result is that the responsitivity of the detector is increased, leading to absorption coefficients that are apparently negative at low frequencies. The readjustment typically comes to 10% of the value of the absorption coefficient at 50 cm^{-1}.

The experimental data are shown as circles in all of the figures. The solid and variously dashed curves are calculated ones, as will be described shortly.

Figure 1 shows the results for both sludge samples. The copper data are plotted as solid circles; the lead as open circles. The two samples appear very similar. The absorption coefficient is very small at low frequencies, bends up near 10 cm^{-1} and increases nearly linearly at high frequencies. Even though the data were taken at 4.2 K, well below the bulk superconducting transition temperature of lead, there is no evidence of any reduction of the absorption below the bulk energy gap of 22 cm^{-1}. This curve is indistinguishable from others taken at 9, 20, or 1.2 K. The same is true for copper. The straight part of the curve extrapolates to zero at 10 ± 1 cm^{-1} for both materials. The first specimens measured were sludges. We were never confident that all residual acetone had been removed from the particles, and acetone is a strong absorber in the far infrared. When the better controlled particle smokes became available we stopped studying sludge. All of the remaining data refers to particle smokes.

The absorption coefficients at 4.2 K of both Cu 2 and Cu 3 are shown in Fig. 2. Cu 2 has an average diameter of 70 Å and Cu 3 of 270 Å. Cu 2 has a horizontal (zero) value at low frequencies and then rises nearly linearly at high frequencies. The linear section extrapolates to zero at 19 ± 1 cm^{-1}. Cu 3 is already rising linearly at the lowest frequencies. This section of data extrapolates to zero near zero frequency. There is a big bend at 30–

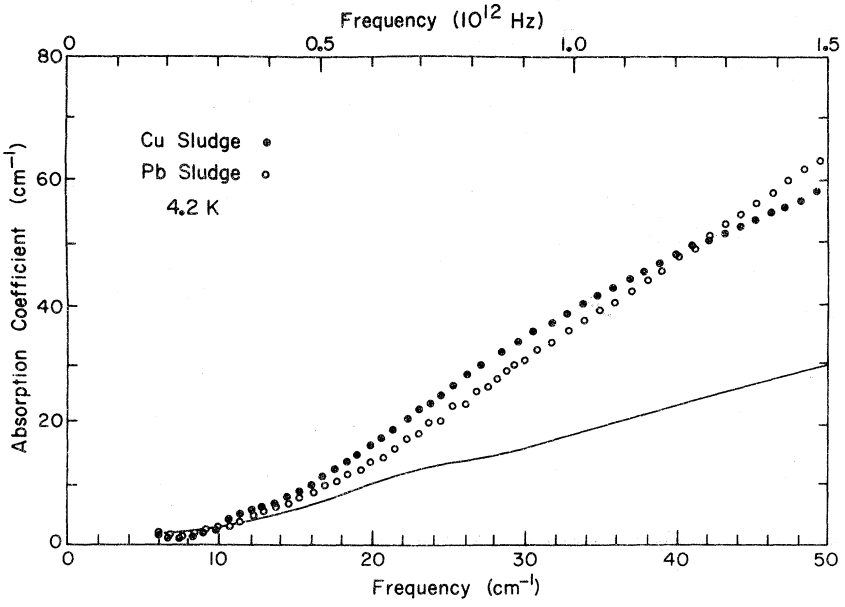

FIG. 1. Measured absorption coefficient for copper sludge (full circles) and lead sludge (open circles) vs frequency. The solid line is calculated from the orthogonal ensemble for the copper sludge. The samples were at 4.2 K.

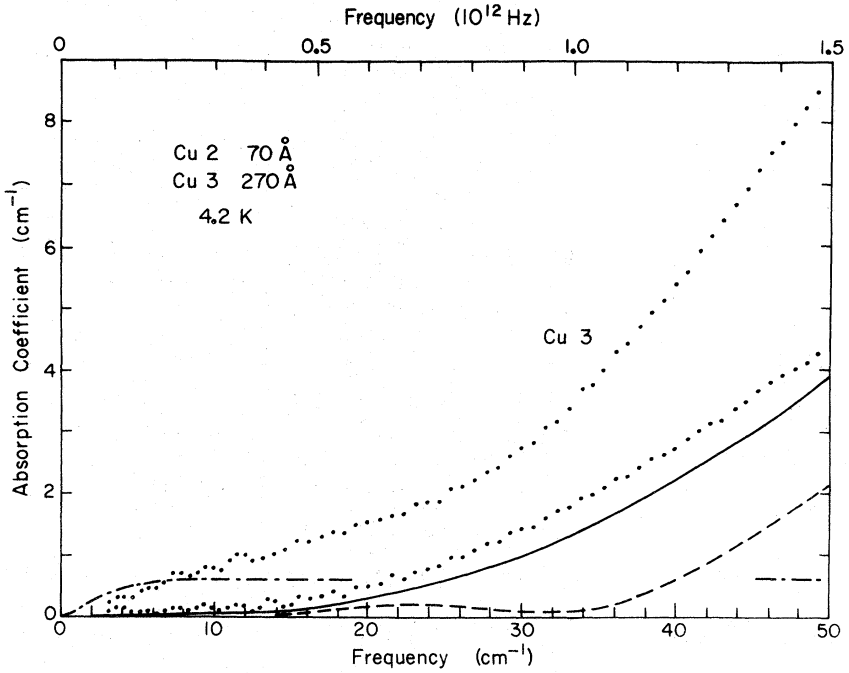

FIG. 2. Measured absorption coefficient for Cu 2 and Cu 3 vs frequency. The solid line is calculated from the orthogonal ensemble for Cu 2, the dashed line from the symplectic ensemble for Cu 2, and the dot-dashed line from the orthogonal ensemble for Cu 3. See Table I for sample identification.

35 cm^{-1} and then it continues linearly but with a larger slope. The larger particles absorb more at a given frequency than the smaller ones by about a factor of 2.

In Fig. 3 is shown the data for 150-Å aluminum, Al 1, at 4.2 K. This is a high-resolution run ($r = 0.4$ cm^{-1}) and there is a large amount of structure. This consists of short straight sections separating three cycles of large oscillations. The oscillations are at 2.3-cm^{-1} intervals. The pattern repeats at 8.1-cm^{-1} intervals. There are error bars in a few places showing the noise on the data, which is much smaller than the oscillations. If the upper section is extrapolated to zero, ignoring the oscillations, it intersects at 13 ± 1 cm^{-1}. The spectrum shown was taken at 4.2 K but there

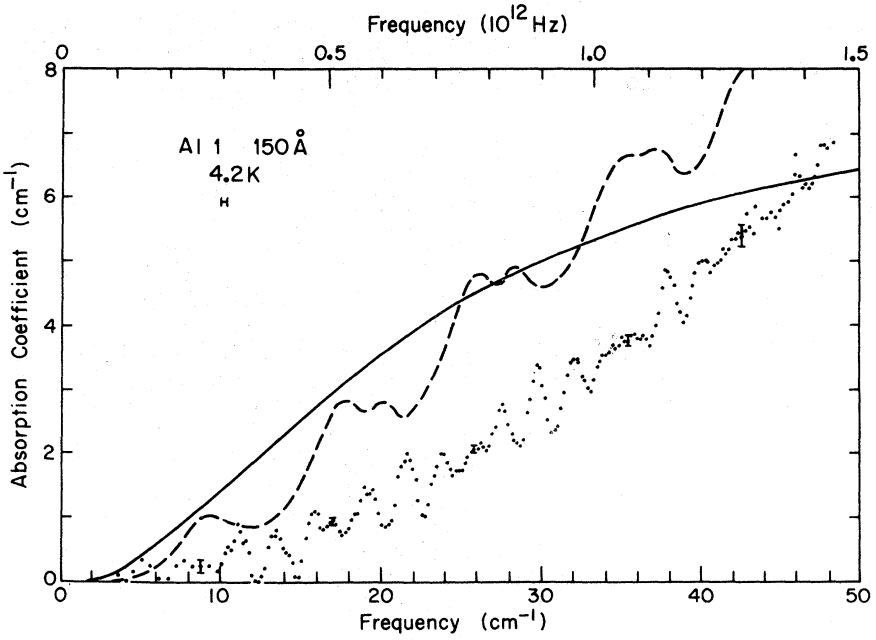

FIG. 3. Measured absorption coefficient for Al 1 vs frequency. The solid line is calculated from the orthogonal ensemble and the dashed line from the symplectic ensemble. The instrumental resolution is shown.

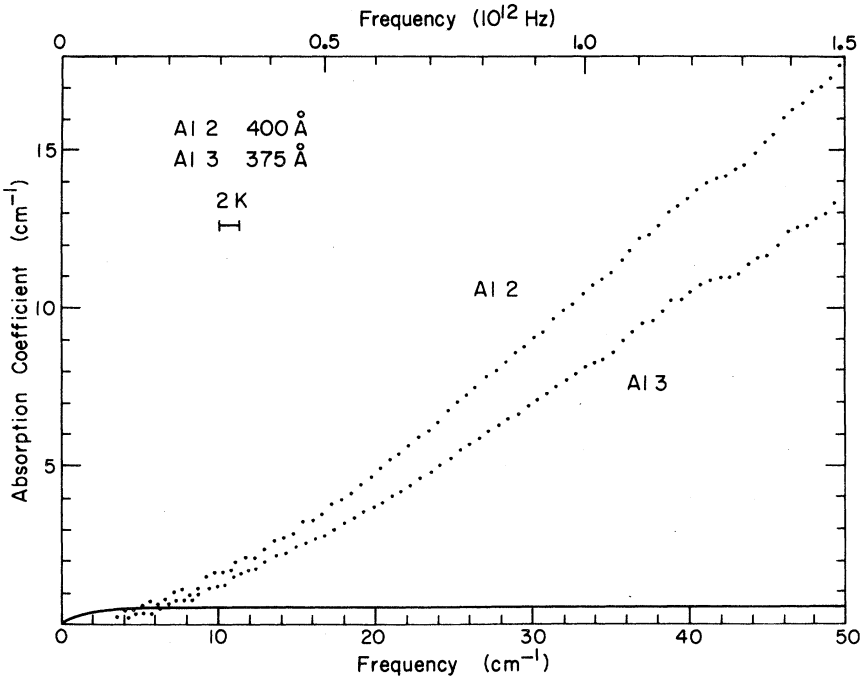

FIG. 4. Measured absorption coefficient for Al 2 and Al 3 vs frequency. The solid line is calculated from the orthogonal ensemble and applies to either specimen. The instrumental resolution is shown.

is no noticeable difference between this and one at 2 K.

Figure 4 displays the results for the other two aluminum samples, Al 2 (400 Å) and Al 3 (370 Å), at 2 K this time. Both have absorption coefficients considerably larger than Al 1. Neither absorption coefficient levels out at low frequencies. Both extrapolate to zero below the lowest frequency measured. The resolution is lower than in Fig. 2 ($\gamma = 1.5\ \mathrm{cm}^{-1}$) but would show any similar structure, if such existed.

Figure 5 gives the results for 140-Å tin particles, Sn 1 at two temperatures, 4.2 and 1.2 K. It shows the usual behavior, with the straight upper section extrapolating to zero at $13 \pm 1\ \mathrm{cm}^{-1}$. There are some very small oscillations here, with period 8 to 9 cm^{-1}. The low-frequency end is almost flat. The inset at the upper left shows the absorption in

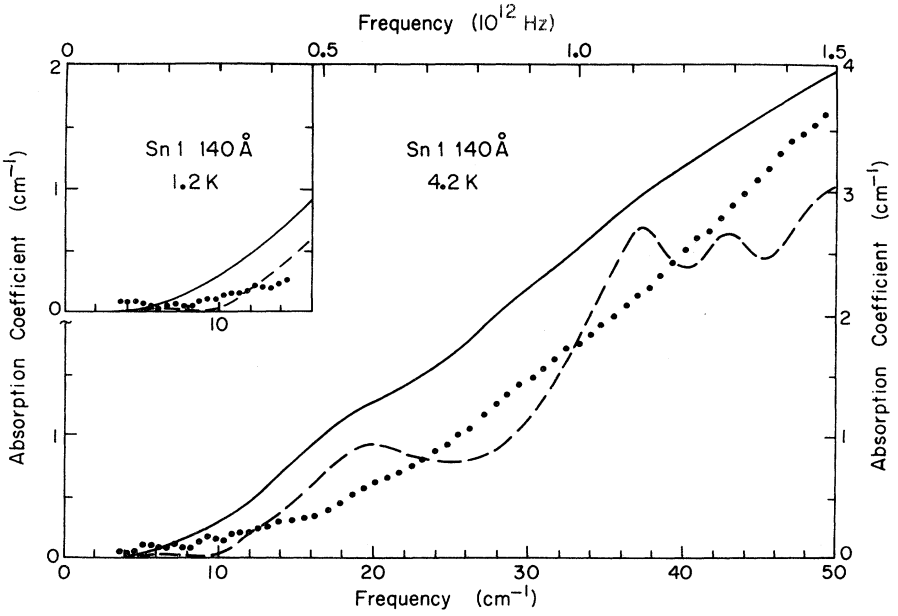

FIG. 5. Measured absorption coefficent for Sn 1 vs frequency. The main drawing is the data at 4.2 K; the small insert shows the results at 1.2 K. The solid lines are calculated from the orthogonal ensemble and the dashed lines from the symplectic ensemble.

the same region at 1.2 K. The superconducting transition temperature of tin is 3.7 K and the energy gap is at 9.3 cm^{-1} in bulk or thin-film tin samples. Any effect of the superconductivity should show up near or below this frequency. The two curves at the two temperatures are almost identical point by point; no effect due to the superconductivity can be seen. The data for Sn 2 were much the same.

Figure 6 shows the results for carbon particles, 90 Å in diameter. This is intended to show the behavior of nonmetallic particles. It shows a smooth almost linear increase ($\sim \omega^{3/2}$) in absorption coefficient with frequency. This is quite different from the absorption in metallic particles of similar size; there is no flat region at low frequencies and the absorption coefficient is smaller than any metallic particle. Since the carbon was handled in the same fashion as the metallic particles any effects from adsorbed gasses on the surfaces should show up here; if there are any they add no structure to the absorption coefficient. The data were taken at 2 K, but there is no difference between this and 1.2 and 4.2 K.

IV. CALCULATIONS

The problem of finding the absorption coefficient for these small particles divides into three parts: (i) calculating the effective dielectric function of a medium containing a large number of particles (electrostatics), (ii) finding the relation between the internal field and the applied external field including depolarization effects (electrostatics), and (iii) calculating the linear response of the system to the internal electric field (quantum mechanics). The electrostatics parts may be done after making three simplifying assumptions (a) Scattering is not important, so that the medium appears homogeneous to the radiation. (b) There is no interaction among the particles, e.g. we ignore completely the dipolar fields of the particles themselves. (c) The particles are isotropic spheres of uniform size having diameters smaller than their skin depth or the wavelength of the far infrared radiation ($D \ll \delta, \lambda$).

The effective medium problem was originally solved by Maxwell-Garnett[14] and has been discussed recently by Genzel and Martin[15]; by Rieder, Ishigame, and Genzel[16]; and by Barker.[17] It is convenient to describe the material by a complex susceptibility χ as its properties are generally manifested via the polarization of the particle. The particle has a dipole moment $\vec{p} = \Omega\vec{P} = \Omega\chi\vec{E}_{in}$, where $\vec{P}$ is the polarization vector and $\vec{E}_{in}$ is the electric field inside the particle. The dipole moment is also given by $\vec{p} = \alpha_p\vec{E}_{ext}$, where α_p is the polarizability of the particle and $\vec{E}_{ext}$ the applied electric field.

From the solution of the boundary value problem of a sphere having electric susceptibility χ in an applied field $\vec{E}_{ext}$ (see for example Jackson[18]), the internal and external fields can be related. The external field causes charges to collect on the surface which create a depolarizing field leading to a reduction in the field inside the sphere. The result is

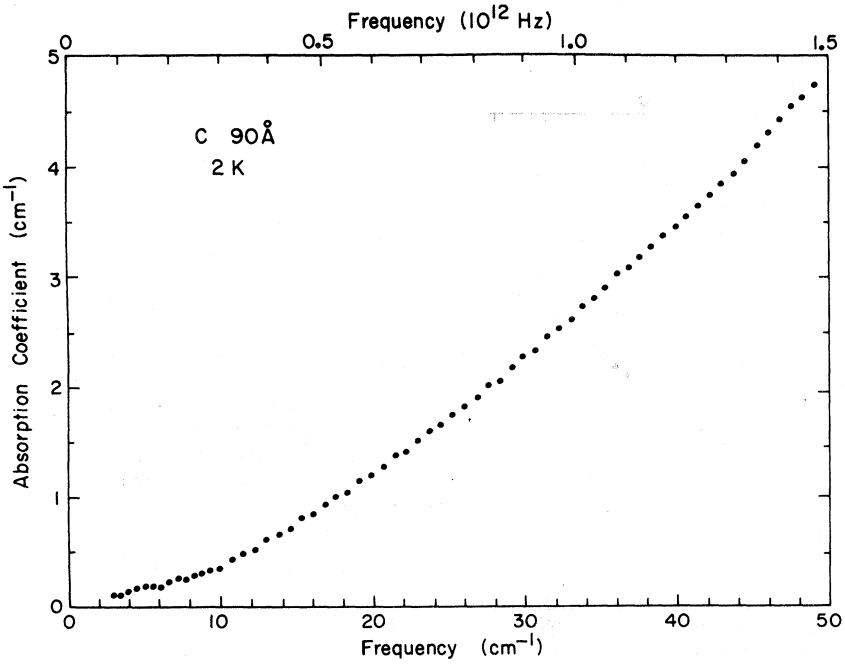

FIG. 6. Measured absorption coefficient for carbon vs frequency. The sample temperature is 2 K.

$$\vec{E}_{in} = \vec{E}_{ext} - \tfrac{4}{3}\pi \vec{P} \quad , \tag{2}$$

$$\alpha_p = \Omega\chi/(1 + \tfrac{4}{3}\pi\chi) \quad . \tag{3}$$

The composite medium is most easily discussed in terms of its average dielectric function ϵ_{av}, such that $\vec{D}_{av} = \epsilon_{av}\vec{E}_{av}$, where $\vec{D}_{av}(\vec{E}_{av})$ is the volume average displacement vector (electric field) in the medium. If f is the fraction of the medium occupied by the particles (the rest being vacuum) then these fields are

$$\vec{E}_{av} = (1-f)\vec{E}_{ext} + f\vec{E}_{in} \quad , \tag{4}$$

$$\vec{D}_{av} = (1-f)\vec{E}_{ext} + f(\vec{E}_{in} + 4\pi\vec{P}) \quad . \tag{5}$$

Equations (2)–(5) may be solved to find

$$\epsilon_{av} = 1 + 4\pi(f/\Omega)\alpha_p/[1 - \tfrac{4}{3}\pi(f/\Omega)\alpha_p] \quad . \tag{6}$$

This is just the expression for the dielectric function of a gas of polarizable molecules, as given in, again, Jackson.[18]

If χ is complex, $\chi = \chi_1 + i\chi_2$, then $\epsilon_{av} = \epsilon_{av1} + i\epsilon_{av2}$ and

$$\epsilon_{av1} = 1 + \frac{4\pi f[\chi_1 + \frac{4}{3}\pi(1-f)(\chi_1^2+\chi_2^2)]}{1 + \frac{8}{3}\pi(1-f)\chi_1 + (\frac{4}{3}\pi)^2(1-f)^2(\chi_1^2+\chi_2^2)} \quad , \tag{7}$$

$$\epsilon_{av2} = \frac{4\pi f\chi_2}{1 + \frac{8}{3}\pi(1-f)\chi_1 + (\frac{4}{3}\pi)^2(1-f)^2(\chi_1^2+\chi_2^2)} \, . \tag{8}$$

The absorption coefficient of the medium is given by

$$\alpha(\omega/c)[\,2(\epsilon_{av1}^2 + \epsilon_{av2}^2)^{1/2} - 2\epsilon_{av1}\,]^{1/2} \tag{9}$$

Using Eqs. (7)–(9) and an expression for the dielectric susceptibility of a particle, the absorption coefficient of the medium containing the particles may be found.

The quantum-mechanical problem of the electromagnetic response of a particle with energy level spacing given by Eq. (1) was solved by Gor'kov and Eliashberg[4] with emendations by Strassler, Rice, and Wyder[19] and by Lushnikov and Simonov.[20]

Gor'kov and Eliashberg did their calculation for the three ensembles derived by Dyson.[3] The applicability of the ensembles depends on the strength of the spin-orbit coupling. In the case of small spin-orbit coupling L and S are good quantum numbers and the orthogonal ensemble applies, for large spin-orbit coupling L and S are not good quantum numbers and the symplectic ensemble is used, and for a large magnetic field and large spin-orbit coupling the unitary ensemble is used. When the spin orbit coupling is large there are big interactions among the levels; they are expected to repel each other and fall into a more uniform arrangement; in this case a more periodic behavior is expected than in the orthogonal ensemble.

The result is that the dielectric susceptibility is (for small electric fields and the diameter D less than the bulk mean free path)

$$\chi = \frac{1}{20\pi}\frac{e^2}{\Delta D} + \frac{139}{1200\pi^2}\frac{e^2}{h v_F}A(\omega) \quad , \tag{10}$$

where the first term is the static susceptibility and is frequency independent and v_F is the Fermi velocity. The function $A(\omega)$ is determined by the ensemble average used.

For light metals ("small" spin-orbit coupling) the orthogonal ensemble applies. Expressed in terms of the integral sine $\mathrm{Si}(\chi)$ and integral cosine $\mathrm{Ci}(\chi)$,

$$A(\omega) = 2 - \frac{\Delta}{\pi\hbar\omega}\sin\frac{2\pi\hbar\omega}{\Delta} - \frac{2\Delta}{\pi\hbar\omega}\mathrm{Ci}\left(\frac{\pi\hbar\omega}{\Delta}\right)\left(\sin\frac{\pi\hbar\omega}{\Delta} - \frac{\pi\hbar\omega}{\Delta}\cos\frac{\pi\hbar\omega}{\Delta}\right)$$
$$+ i\left[\frac{2\pi\hbar\omega}{\Delta} - \frac{\Delta}{\pi\hbar\omega} + \frac{\Delta}{\pi\hbar\omega}\cos\frac{2\pi\hbar\omega}{\Delta} - \frac{\Delta}{\pi\hbar\omega}\mathrm{Si}\left(\frac{\pi\hbar\omega}{\Delta}\right)\left(\sin\frac{\pi\hbar\omega}{\Delta} - \frac{\pi\hbar\omega}{\Delta}\cos\frac{\pi\hbar\omega}{\Delta}\right)\right] \, .$$

For heavy metals ("large" spin-orbit coupling) the symplectic ensemble is used:

$$A(\omega) = 2 - \frac{\Delta}{2\pi\hbar\omega}\sin\frac{2\pi\hbar\omega}{\Delta} - \frac{\Delta}{\pi\hbar\omega}\left[\frac{\pi}{2} + \mathrm{Si}\left(\frac{\pi\hbar\omega}{\Delta}\right)\right]\left(\cos\frac{\pi\hbar\omega}{\Delta} + \frac{\pi\hbar\omega}{\Delta}\sin\frac{\pi\hbar\omega}{\Delta}\right)$$
$$+ i\left\{\frac{\pi\hbar\omega}{\Delta} - \frac{\Delta}{\pi\hbar\omega}\sin^2\frac{\pi\hbar\omega}{\Delta} + \frac{\Delta}{\pi\hbar\omega}\left[\frac{\pi}{2} + \mathrm{Si}\left(\frac{\pi\hbar\omega}{\Delta}\right)\right]\left(\frac{\pi\hbar\omega}{\Delta}\cos\frac{\pi\hbar\omega}{\Delta} - \sin\frac{\pi\hbar\omega}{\Delta}\right)\right\} \, .$$

In the case of the symplectic ensemble there are large periodic variations in the susceptibility with frequency while the orthogonal ensemble yields a relatively smooth function.

The static susceptibility in Eq. (10) is quite large and led Gor'kov and Eliashberg to predict a large polarizability for small particles. Experiments by Meier and Wyder[21] and by Dupree and Smithard[22] produced no such effect. This led Strassler, Rice, and Wyder to make their comment, the main point of which was that Gor'kov and Eliashberg had mistaken the dielectric susceptibility for the polarizability. This is equivalent to ignoring the depolarizing field and writing

Eq. (2) as $\vec{E}_{in} = \vec{E}_{ext}$.

The classical (Drüde) expression for the dielectric susceptibility of a metal is

$$\chi = i\sigma_0/\omega(1 - i\omega\tau) \quad , \tag{11}$$

where σ_0 is the dc conductivity and τ is the electron relaxation time. Putting this into Eqs. (3) and (6) yields

$$\epsilon_{av} = 1 + \frac{4\pi f \sigma_0/\tau}{\frac{4}{3}\pi(1-f)(\sigma_0/\tau) - \omega^2 - i\omega/\tau} \quad . \tag{12}$$

This is the dielectric function of a Lorentzian oscillator of width $1/\tau$ and resonant frequency $\omega_0 = [(\frac{4}{3}\pi)(1-f)\sigma_0/\tau]^{1/2}$. For these particles, $f \sim 0.1$ and, taking the mean free path as the diameter and $v_F \sim 10^8$ cm/sec, $1/\tau \sim 10^{14}$ sec^{-1}. For typical metals $\sigma_0 \sim 10^{17}$ sec^{-1}, so $\omega_0 \sim 10^{16}$ sec^{-1}. This is well above far-infrared frequencies for which $\omega \lesssim 10^{13}$ sec^{-1}. The dielectric function becomes

$$\epsilon_{av} = 1 + \frac{3f}{1-f} + i\frac{9\omega f}{4\pi(1-f)\sigma_0} \quad . \tag{13}$$

The real part of ϵ_{av}, in this limit, turns out to be independent of the properties of the particle. This is a consequence of the nearly complete screening of the field inside. On substitution of Eq. (13) into Eq. (9) the absorption coefficient is found to be

$$\alpha = \frac{9\omega^2 f}{4\pi c\sigma_0(1 + f - 2f^2)^{1/2}} \quad . \tag{14}$$

It is worthwhile to briefly discuss the simplifying assumptions made at the beginning of this section. If the diameter of the particle is not utterly negligible compared to (but is still less than) the skin depth, there will be a loss from its magnetic polarization (eddy currents). In a time varying field the particle has a definite magnetization. This problem has been discussed nicely by Landau and Lifshitz.[23] The absorption coefficient due to eddy-current losses is proportional to the imaginary part of the magnetic polarizability $\alpha_{m2} = D^2\omega\sigma_0/40c^2$. It is

$$\alpha = \tfrac{1}{10}\pi f \omega^2 D^2 \sigma_0/c^3 \quad . \tag{15}$$

This loss is in parallel with that from electric polarization so that the total absorption in the classical model is the sum of Eqs. (14) and (15),

$$\alpha = f\frac{\omega^2}{c}\left(\frac{9}{4\pi\sigma_0(1 + f - 2f^2)^{1/2}} + \frac{\pi D^2\sigma_0}{10c^2}\right) \quad . \tag{16}$$

Using $\sigma \sim 10^{17}$ sec^{-1}, $f \sim 0.1$, the second term dominates for diameters larger than 50 Å.

Rayleigh[24] was the first to solve the problem of scattering by small particles. The particles have a dipole moment $\vec{p} = \alpha_p \vec{E}_{ext}$ with α_p given by (3). Since $\vec{E}_{ext}$ has time dependence $e^{-i\omega t}$, the particle is an oscillating dipole, whose dipole radiation corresponds to the scattered light. The total power radiated is $P = \frac{1}{3}\omega^4|\vec{p}|^2/c^3$. The cross section S is this power divided by the incident energy flux density $c|\vec{E}_{ext}|^2/8\pi$,

$$S = (8\pi\omega^4/3c^4)|\alpha_p|^2 \quad .$$

From Eqs. (3) and (11) and the values of σ_0, ω, and τ used above, $|\alpha_p| = 3\Omega/4\pi$ to within a part in 10^5, and $S \sim 10^{-27}$ cm^2. The angular distribution of the scattered radiation exhibits a characteristic $\sin^2\theta$ dependence, where θ is measured relative to the incident light. If we consider radiation in any direction but $\theta = 0$ to be lost to the detector, then the absorption coefficient due to scattering is $\alpha = NS/V = fS/\Omega$. Any multiple scattering (subsequent scattering of already scattered light by another particle in the composite medium) can only affect the detector by increasing the intensity at $\theta = 0$. The upper limit for the absorption coefficient due to scattering is

$$\alpha = f\omega^4 D^3/4c^4 \quad .$$

For a 100-Å-diam particle at $\omega \sim 10^{13}$ sec^{-1} and with $f \sim 0.1$, $\alpha \sim 10^{-9}$ cm^{-1}. This is probably negligible.

The dipolar fields will contribute to ϵ_{av} only if the field from a given particle is significant at the surfaces of its neighbors. This depends on the polarizability and the filling factor. If r is the mean distance between particle centers then r^3 is the volume allotted to one particle and $r = (\Omega/f)^{1/3}$. The field from the dipole moment $\vec{p} = \alpha_p \vec{E}_{ext}$ of a particle at the nearest surface of a neighbor at $\vec{r}$ is

$$\vec{E}_{dip} = \frac{3(\vec{n}\cdot\vec{E}_{ext})\vec{n} - \vec{E}_{ext}}{[(\Omega/f)^{1/3} - (3\Omega/4\pi)^{1/3}]^3}\,\alpha_p \quad ,$$

where $\vec{n}$ is a unit vector in the direction of $\vec{r}$ and the second term in the denominator is a complicated way of writing the particle radius. For the purposes of an estimate we will take $\vec{n}$ along $\vec{E}_{ext}$ and $\alpha_p = (3/4\pi)\Omega$. Then

$$\vec{E}_{dip} = \frac{3f}{2\pi[1 - (3f/4\pi)^{1/3}]^3}\,\vec{E}_{ext} \quad .$$

The dipolar fields may be ignored to the extent that f is small with respect to unity. As f is increased they suddenly become quite important. For $f \sim 0.04$ (most of the specimens studied here) $\vec{E}_{dip} \sim 0.04\vec{E}_{ext}$. $\vec{E}_{dip} = \vec{E}_{ext}$ when $f = 0.35$.

We are now in a position to discuss the curves generated from the above equations. In Fig. 1 the solid line is the absorption coefficient calculated for the orthogonal ensemble in the copper sludge. The result for lead would be slightly below the curve shown. Both calculations are about a factor of 2 smaller than the data points. In Fig. 2 the solid line is for the orthogonal ensemble in Cu 2, the dashed line is for the symplectic ensemble in

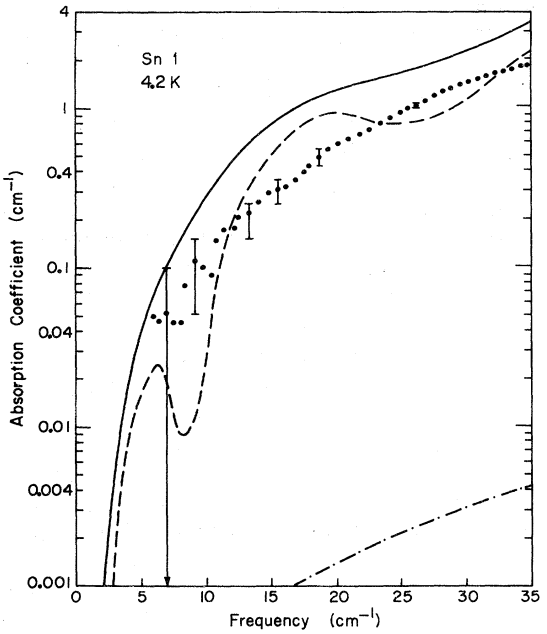

FIG. 7. Absorption coefficient (on a logarithmic scale) for Sn 1 vs frequency. The solid line is calculated from the orthogonal ensemble, the dashed line from the symplectic ensemble and the dot-dashed line from the classical (Mie) theory.

Cu 2 and the dot-dashed line is for the orthogonal ensemble in Cu 3. The last one has been suppressed where it would have passed through any of the curves for Cu 2. The orthogonal ensemble gives both the shape and magnitude of the absorption coefficient for Cu 2 very well. It does however, very poorly for Cu 3. This is likely a case where the dielectric formalism no longer applies. In Fig. 3 the solid line shows the orthogonal ensemble and the dashed line the symplectic ensemble for Al 1. Both are above the measured data, but the symplectic ensemble gives the over-all shape well and, remarkably, suggests the fine structure. In Fig. 4 the solid line shows the orthogonal ensemble, applicable to either Al 2 or Al 3. This misses badly; probably a breakdown of the dielectric formalism. In Figure 5 the solid lines show the orthogonal ensemble and the dotted lines show the symplectic ensemble for Sn 1. The orthogonal ensemble gives the shape of the curve pretty well and the average of the symplectic ensemble gives the magnitude.

In all of the figures the absorption coefficient calculated from Eq. (16), the classical theory, would be on the x axis. In order to show this, we have plotted the data for Sn 1 on a logarithmic scale in Fig. 7. The full circles are the data points, some have error bars on them. The solid line is calculated from the orthogonal ensemble, the dashed line from the symplectic ensemble, and the dot-dashed line from the classical theory. The classical theory gives the over-all shape pretty well at higher frequencies but fails miserably on predicting the magnitude of the absorption.

V. DISCUSSION

Table II gathers together the important points from the measurements. The first column gives the sample designation, the second its average diameter, the third the calculated value of Δ from Eq. (1), the fourth the spread in Δ from the variation in the diameter, the fifth the intercept of the more or less straight section with the x axis which is an experimental value for Δ, the sixth the measured absorption coefficient at 40 cm^{-1}, and the last this absorption coefficient divided by f. Since the absorption coefficient more or less scales with f this might help to eliminate any effects of different packing densities on the data.

Considering the strong dependence of Δ on the diameter, the rough agreement of most of the samples between the calculated and experimental value is quite satisfactory. In the copper smoke the calculated value comes out high; in the aluminum and tin somewhat low. The two sludge samples, surprisingly, were very close.

TABLE II. Data on small particles.

Sample	Diameter (Å)	Calculated energy-level spacing (cm^{-1})	Spread (cm^{-1})	Measured energy-level spacing (cm^{-1})	Absorption at 40 cm^{-1} α (cm^{-1})	Absorption at 40 cm^{-1} α/f (cm^{-1})
C	90	•••	•••	•••	3.4	79
Pb sludge	100	15	7–40	10±1	43	360
Cu sludge	100	11	5–30	10±1	44	370
Cu 2	70	31	20–50	19±1	2.7	97
Cu 3	270	0.55	0.4–1	<3	5.3	190
Al 1	150	4.2	3–5	13±1	5.0	120
Al 2	400	0.22	0.2–0.3	<3	14	340
Al 3	375	0.27	0.2–0.3	<3	10	260
Sn 1	140	8.9	7–12	13±1	2.4	130

Although the absorption coefficients at 40 cm^{-1} do not follow any pattern, dividing them by the filling factor f does bring them into order with a couple of exceptions. This number α/f is approximately proportional to the absorption per particle rather than the absorption per centimeter of the composite medium and is shown in Fig. 8. This is a log-log plot of the ratio of coefficient to filling factor versus diameter for the particles. These data are shown as crosses in the figure and a dashed line is drawn through them. The line has a slope of $\frac{2}{3}$ meaning that the absorption increases as $D^{2/3}$. Also in Fig. 8 are the same data with the number for carbon subtracted off. These are shown as circles and fall into a somewhat straighter solid-line slope $\frac{3}{2}$ ($\alpha \sim D^{3/2}$). Subtracting off the value for carbon is done in an attempt to eliminate the absorption from nonmetallic causes and is of some value if the absorption due to carbon is independent of diameter. This is a somewhat shaky assumption.

The major anomaly in the data is the structure in Al 1 which consists of very regular well-resolved oscillations at 2.3-cm^{-1} intervals modulated by ones at 8.1 cm^{-1} intervals, producing a beating effect. In Fourier-transform spectroscopy one must always be on guard against such behavior because it can be caused by two bad points in the interferogram or by two interference patterns in the sample. Both would be Fourier transformed into such a pattern. Neither of these is the case in Al 1. The pattern was visible in all of the spectra taken on Al 1 during two different runs separated by a period of a month and on none of the other samples run simultaneously. Because nine interferograms were recorded for Al 1 and because the pattern was visible in all of them it was not due to two bad points in the interferogram. If it was due to an interference pattern, the pattern could only be in the Al 1 sample itself. Al 1 was one of five samples on a brass rotator disk which were placed in the far-infrared beam successively. As the pattern was not observed in any of the other samples it must be localized in Al 1. The samples were mounted as follows: a piece of 0.001-in.-thick polyethylene was placed over the hole in the brass sample rotator, a short section (perhaps 1 mm thick) of brass or nalgene tubing was put on it and the powder poured in, another sheet of polyethylene was used to cover the powder and the whole assembly held down with a piece of brass shim stock screwed to the rotator. It seems inconceivable that the two polyethylene sheets separated by the powder would be sufficiently flat and parallel to cause standing waves *between* them. We conclude that the structure seen in Fig. 3 is a property of the powder itself. The calculated absorption coefficient for the symplectic ensemble is suggestive of the data, even to showing a beating effect. It is different in detail, however. The period of the oscillations is just about half of the calculated mean energy-level spacing in Table II. Al 1 had the smallest percentage variation in size of any of the samples. It is the sample in which structure is most likely to be found.

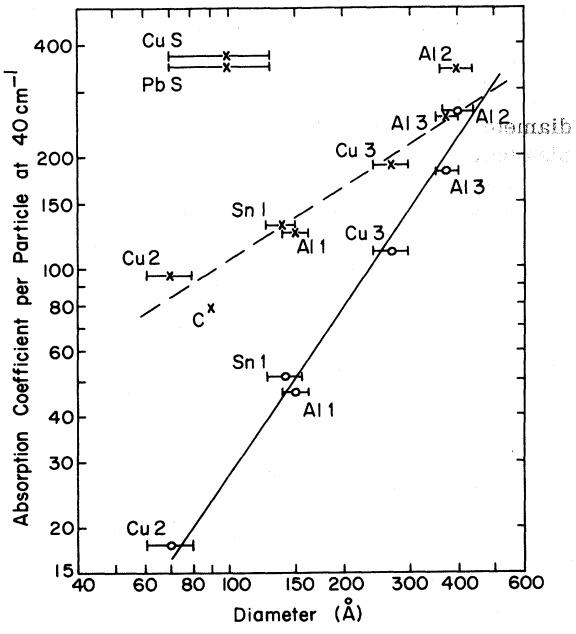

FIG. 8. Absorption coefficient at 40 cm^{-1} divided by the filling factor vs particle diameter. See Table I for sample identification.

As might be guessed, Al 2 was an attempt to duplicate the results of Al 1 with another sample. The particle size turned out to be too large and too uneven in size. For the present Al 1 must stand alone and is not completely understood.

The question of possible interaction among particles is a difficult one. Although the mean separation between particles is great enough in all but the sludge samples to make interactions negligible, the particles are not in any medium. Many of them may be much closer than the mean separation $r = (f/\Omega)^{1/3}$. The particles, however, do have an oxide layer on their surfaces. Electron-microscope diffraction pictures of the copper particles show a double-ring pattern typical of fcc copper and, outside this, a pattern identified as simple cubic Cu_2O. The density of this line is less than the copper lines, implying that perhaps 10% of the particle is composed of the oxide. There is probably another layer of absorbed atmospheric gasses surrounding this. These will help to keep the particles separated. As mentioned above, the particles are observed to have very low dc conductivity

and to be microscopically isolated as far as their static magnetic properties are concerned.[10] Infrared experiments by Rieder, Ishigame, and Genzel[16] on CdO smoke with $f \sim 0.03$ and by Barker[17] on localized modes from impurities in polar semiconductors with f in the range 0.02 to 0.1 were both successfully analyzed using dielectric functions of the form of Eq. (6). We feel confident in doing the same.

There is another point to be made concerning the oxide layer. It should be completely transparent at the far infrared frequencies of interest. It will reduce the diameter of the metallic small particle though. Two layers of oxide on the surface will reduce the diameter of the metal by 14 Å or so. This is not an insubstantial amount in the smaller particles. But, it is likely that the electrons can easily penetrate two layers of oxide (this being a typical thickness in tunnel junctions) to reach the surface so that the volume of the small particle will be the same whether oxidized or not. The density of the electrons will be reduced proportionally to the number of electrons bound to oxygen atoms. The effect of the oxide will be to increase the energy level spacing.

One unexpected result of these experiments was the total lack of temperature dependence in the samples, at the temperatures studied. The copper and lead sludge samples were studied at 1.2, 4.2, 9, and 20 K; the Cu 1 sample at 4.2, 9, and 25 K; Al 1 at 2 and 4.2 K; and Sn 1 and Sn 2 at 1.2 and 4.2 K. None of these showed any effects of temperature although a previously unknown temperature-dependent absorption in quartz was found during the course of these investigations. In particular, the absorption of the superconducting samples did not change at all when cooled well below the bulk metal transition temperature. This was unexpected since the appearance of a superconducting energy gap in an array of small particles should lead to a reduced absorption at this gap and nearly zero absorption at frequencies below it. This is not seen in any of the samples below their superconducting transition temperatures.

There are two reasons why the size of the small particles might be expected to affect superconducting behavior. If the diameter of the particle is on the order of 100 Å, then the mean energy-level spacing is on the order of kT_c. Further, if the diameter of the particle is less than the coherence length of the electrons, the long range order of the system is restricted and thermal fluctuations can also become very important. Anderson[25] and Strongin *et al.*[26] have considered the spacing effect, in the absence of fluctuations, and have concluded that if $\Delta > 2kT_c$, there is no superconductivity. (The effective transition temperature of the particles is zero.) The particles exhibit the bulk transition temperature when $\Delta \leq kT_c$.

Schmid[27] has discussed the existence or lack thereof of the energy gap in a superconductor without long-range order. His conclusion is that there is no energy gap; the density of electron states at $T=0$ rises linearly from zero at zero frequency to a peak near the BCS energy gap after which it falls off to the normal state value. This discussion ignores any influence of finite energy level spacing.

Shmidt,[28] Muhlschlegel *et al.*,[29] and Patton,[30] among others, have all considered the effect of thermal fluctuations on the superconducting properties of small particles. The common conclusion is that thermal fluctuations have a very strong effect on particles whose diameter is much less than the superconducting coherence length. Muhlschlegel *et al.* have also included a discussion of finite energy level effects and have concluded that until $\Delta \approx kT_c$ the effect is not significant.

Perhaps the most directly applicable work is that of Patton who has calculated the density of states for such a small particle "zero-dimensional" system. He finds that the major effect of fluctuations is to smooth out the BCS energy-gap structure in a critical temperature region centered about T_c. Only at temperatures well below this critical region does the standard BCS gap clearly emerge in the small-particle density of states. The width of the critical region grows as the particle diameter decreases, eventually extending over the entire temperature range below T_c. It is interesting to note that this is predicted to occur at approximately the same particle diameter which gives a mean level spacing $\Delta = kT_c$. This suggests that when the point is reached where level spacing effects become important, thermal effects will have already greatly changed the nature of superconductivity in these particles.

Experimentally, the superconducting diamagnetic susceptibility has been extensively studied in very small aluminum particles.[10] These experiments show that the thermodynamic fluctuation theories do indeed give a very accurate description of the superconductivity in small particles, at least for particle diameter of 200 Å or greater. The results indicate, although indirectly, that fluctuations do change the BCS gap structure as the particle diameter decreases. The infrared absorption studies reported here now give direct evidence that for superconducting particles of diameter ~ 100 Å and $\Delta \simeq kT_c$ the energy gap structure in the density of states is either very much attenuated or is completely absent.

For all the samples investigated the absorption was found to increase with frequency. Most of the samples studied were optimized in thickness for the 10–40-cm^{-1} region and did not transmit suffi-

cient far infrared at higher frequencies to permit measurement of α there. One very thin copper-sludge sample was measured in the near infrared at room temperature; it showed a continuing increase in the absorption with increasing frequency between 1000 and 4000 cm^{-1} (10- to 2.5 μm wavelength). At these frequencies, classical scattering, which increases as ω^4, would be expected to be the dominant loss mechanism. In the visible at room temperature almost all of the small particle specimens are black. Some of the larger ones show a slight blue-grayish tinge.

VI. SUMMARY AND CONCLUSIONS

These measurements onthe far infrared absorption coefficient of small particles have produced a characteristic spectrum which depends much more on the particle size than on the element of which it is composed. There is very little absorption for frequencies below the mean energy level spacing Δ, a knee near Δ, and a roughly linear rise with frequency above Δ. For the smaller particles, curves generated from the theory of Gor'kov and Eliashberg, with the depolarization field taken care of correctly, give a good description of the data, although clear choices between different statistical ensembles cannot be made. For larger sizes the calculated absorption is far below the measured data. The failure of the calculations is quite abrupt and occurs at about 200-Å diameter. It is probably a result of the assumption of constant internal field no longer being true. The absorption calculated from the classical theory is smaller than the measurements by a factor of 200.

None of the specimens measured showed any temperature dependence, including those made from superconductors at temperatures below the bulk superconducting transition temperature. We must conclude that the superconducting energy gap is either strongly attenuated by thermodynamic fluctuations or is completely absent in these small particles.

We are pleased to acknowledge the advice and assistance of G. J. Dolan and W. P. Halperin during sample preparation.

---

*Work supported by the U. S. Atomic Energy Commission under Contract No. At(11-1)-3151, Technical Report No. COO-3151-38 and by the National Science Foundation under Grant No. GH-38543. Additional support was received from the National Science Foundation under Grant No. GH-33637 through the Cornell Materials Science Center Report No. 2207.

†Present address: Physics Dept., The Ohio State University, Columbus, Ohio 43210.

[1]H. Fröhlich, Physica (Utr.) 6, 406 (1937).
[2]R. Kubo, J. Phys. Soc. Jpn. 17, 975 (1962).
[3]F. J. Dyson, J. Math. Phys. 3, 140 (1962).
[4]L. P. Gor'kov and G. M. Eliashberg, Zh. Eksp. Teor. Fiz. 48, 1407 (1965) [Sov. Phys.-JETP 21, 940 (1965)].
[5]L. Harris and J. K. Beasley, J. Opt. Soc. Am. 42, 127 (1952).
[6]T. Svedberg, Kolloid-Z. Z. Polym. 24, 1 (1919).
[7]M. A. Lunina and Yu. A. Novojhilov, Kolloidn. Jh. 31, 467 (1969).
[8]K. Kimoto and I. Nishida, Jpn. J. Appl. Phys. 6, 1047 (1967).
[9]N. Wada, Jpn. J. Appl. Phys. 6, 553 (1967).
[10]R. A. Buhrman and W. P. Halperin, Phys. Rev. Lett. 30, 692 (1973).
[11]I. G. Nolt, R. D. Kirby, C. D. Lytle, and A. J. Sievers, Appl. Opt. 8, 309 (1969).
[12]H. D. Drew and A. J. Sievers, Appl. Opt. 8, 2067 (1969).
[13]Carbolac Corp., Boston, Mass.
[14]J. C. Maxwell-Garnett, Philos. Trans. R. Soc. 203, 385 (1904); 205, 237 (1906).
[15]L. Genzel and T. P. Martin, Phys. Status Solidi 51, 91 (1972).
[16]K. H. Rieder, M. Ishigame, and L. Genzel, Phys. Rev. B 6, 3804 (1972).
[17]A. S. Barker, Jr., Phys. Rev. B 7, 2057 (1973).
[18]J. D. Jackson, *Classical Electrodynamics* (Wiley, New York, 1962), pp. 114–119.
[19]S. Strassler, M. J. Rice, and P. Wyder, Phys. Rev. B 6, 2575 (1972).
[20]A. A. Lushnikov and A. J. Simonov, Phys. Lett. A 44, 45 (1973).
[21]F. Meier and P. Wyder, Phys. Lett. A 39, 51 (1972).
[22]R. Dupree and M. A. Smithard, J. Phys. C 5, 408 (1972).
[23]L. D. Landau and E. M. Lifshitz, *Electrodynamics of Continuous Media* (Addison-Wesley, Reading, Mass., 1960), Secs. 72 and 73.
[24]Lord Rayleigh, Philos. Mag. (4) XLI, 274 (1871); (4) XLI, 447 (1871); (5) XLVII, 375 (1899).
[25]P. W. Anderson, J. Phys. Chem. Solids 11, 26 (1959).
[26]M. Strongin, R. S. Thompson, O. F. Kammerer, and J. E. Crow, Phys. Rev. B 1, 1078 (1970).
[27]A. Schmid, Z. Phys. 231, 324 (1970).
[28]V. V. Shmidt, *Proceedings of the Tenth International Conference on Low Temperature Physics* (Nauka, Moscow, 1966), Vol. 2B, p. 205.
[29]B. Muhlschlegel, D. J. Scalapino, and R. Denton, Phys. Rev. B 6, 1767 (1972).
[30]B. R. Patton, Ph.D. dissertation (Cornell University, 1973) (unpublished).